Title: CIC-DUX4 oncoprotein drives sarcoma metastasis and tumorigenesis via distinct regulatory programs

Authors: Ross A. Okimoto, Wei Wu, Shigeki Nanjo, Victor Olivas, Yone K. Lin, Rovingaile Kriska Ponce, Rieko Oyama, Tadashi Kondo, and Trever G. Bivona

Supplementary material contains the supplemental methods, 8 figures, and 4 tables.

Supplemental Methods.

Orthotopic and subcutaneous soft tissue xenografts in immunodeficient mice. Six to eight-week old female SCID mice were purchased from Taconic (Germantown, NY).

To prepare cell suspensions for quadriceps injection, adherent tumor cells were briefly trypsinized, quenched with 10% FBS DMEM media and resuspended in PBS. Cells were pelleted again and mixed with Matrigel matrix (BD Bioscience 356237) on ice for a final concentration of $1.0x10^5$ cells/µl. The Matrigel-cell suspension was transferred into a 1ml syringe and remained on ice until the time of implantation.

For orthotopic injection, mice were placed in the right lateral decubitus position and anesthetized with 2.5% inhaled isoflurane. A 0.5 cm surgical incision was made along the posterior medial line of the left hindlimb, fascia and adipose tissue layers were dissected and retracted to expose the quadriceps femoris muscle. A 30-guage hypodermic needle was used to advance through the muscular capsule. For all cell lines, care was taken to inject 10µl ($1.0x10^6$ cells) of cell suspension directly into the left quadriceps femoris. The needle was rapidly withdrawn and mice were observed for bleeding. Visorb 4/0 polyglycolic acid sutures were used for primary wound closure of the fascia and skin layer. Mice were observed post-procedure for 1-2 hours and body weights and wound healing were monitoring weekly. For subcutaneous xenotransplantation, $3.0x10^6$ NCC_CDS1_X3 cells were resuspended in 50% PBS/50% Matrigel matrix and injected into the flanks of immunodeficient mice.

In-vivo bioluminescence imaging. Mice were imaged at the UCSF Preclinical Therapeutics Core starting on post-injection day 7 with a Xenogen IVIS 100 bioluminescent imaging system. Prior to imaging, mice were anesthetized with isoflurane and intraperitoneal injection (IP) of 200µl of D-Luciferin at a dose of 150mg/kg body weight was administered. Weekly monitoring of bioluminescence of the engrafted hindlimb tumors was performed until week 5. Radiance was calculated automatically using Living Image Software following demarcation of the left hindlimb (ROI). The radiance unit of photons/sec/cm2/sr is the number of photons per second that leave a square centimeter of tissue and radiate into a solid angle of one steradian (sr).

Ex-vivo bioluminescence imaging. Mice were injected IP with 200 µl (150mg/kg) of D-Luciferin and subsequently sacrificed at 5 weeks, en-bloc resection of the heart and lungs was performed. The heart was removed and the lungs were independently imaged. Imaging was performed in a 12 well tissue culture plate with Xenogen IVIS 100 bioluminescent imaging.

Cell lines and culture reagents. Cell lines were cultured as recommended by the American Type Culture Collection (ATCC). NIH-3T3, 293T, A673, RD, and RH30 cells were obtained from ATCC. NCC_CDS1_X1 and NCC_CDS_X3 were obtained from Tadashi Kondo at the National Cancer Center, Tokyo, Japan. The presence of the CIC-DUX4 fusion was confirmed through RNAseq analysis using the “grep” command as previously described (Panagopoulos et al, Plos One 2014). All cell lines were maintained at 37 °C in a humidified atmosphere at 5%

CO_2 and grown DMEM 1640 media supplemented with 10% FBS, 100 IU/ml penicillin and 100ug/ml streptomycin. Dinaciclib, palbociclib, SNS-032 were purchased from SelleckChem.

Gene knockdown and over-expression assays. All shRNAs were obtained from Sigma Aldrich. Sequences for individual shRNAs are as follows:

shETV4a: catalog # TRCN0000055132.

shETV4b: catalog # TRCN0000295522.

shCCNE1a: catalog # TRCN0000222722

shCCNE1b: catalog # TRCN0000077776

shCCNE1b: catalog # TRCN0000077777

ON-TARGET plus ETV4, ETV1, ETV5, Scramble, CDK1, CDK2, CDK7, CDK9, CCNE1, and CCNE2 siRNA were obtained from GE Dharmacon and transfection performed with Dharmafect transfection reagent. The HA-tagged CIC-DUX4 plasmid was obtained from Takuro Nakamura (The Cancer Institute of Japanese Foundation for Cancer Research, Tokyo, Japan). Sequence verification was performed using sanger sequencing. The lentiviral GFP-Luciferase vector was a kind gift from Michael Jensen (Seattle Children's Research Institute, Seattle, WA). Fugene 6 transfection reagent was used for all virus production and infection was carried out with polybrene.

Chromatin immunoprecipitation and PCR. CIC null cells (H1975 M1) were transfected with either GFP control, wild-type CIC, or CIC-DUX4 for 48 hours. SimpleCHIP Enzymatic Chromatin IP Kit (Cell Signaling Technology) was used

with IgG (Cell signaling Technology) and CIC (Acris) antibodies per the manufactures protocol.

ETV4 PCR primers were previously described (Okimoto et al., Nature Genetics 2016). The ETV4 primer sequences were as follows:
ETV4_Foward 5'-CGCATCAGACCCAAGACCGTGG-3'
ETV4_Reverse 5'-CCGGAGAGTCGTCCGGCCTGG-3'

CCNE1 PCR primers were designed to flank a tandem TGAATGAA/TGAATGAA sequence from positions -914 to -898 in the CCNE1 promoter. The primer sequences were as follows:
CCNE1_1F CGTCTCGGCCTCCCACAATGCTGGG and
CCNE1_1R CGCGCCTGTGCCTTGGCCTAGAACC.

Chromatin immunoprecipitation – RNA-Seq (ChIPseq) analysis

CIC-DUX4 immunoprecipitation was performed using NCC_CDS_X1 cells. SimpleCHIP Enzymatic Chromatin IP Kit (Cell Signaling Technology) was used with IgG (Cell signaling Technology) and CIC (Acris) antibodies per the manufactures protocol. Paired-end 150bp (PE150) sequencing on a HiSeq platform was subsequently performed. ChIP-Seq peak calls were identified through Mode-based Analysis of ChIP-Seq (MACS).

Luciferase promoter assay. 293T cells were obtained from ATCC. Cells were grown in Dulbecco's modified Eagle Medium (DMEM), supplemented with 10% FBS, 100 IU/ml penicillin and 100ug/ml streptomycin in a 5% CO_2 atmosphere.

Cells were split into a 96 well plate to achieve 50% confluence the day of transfection. LightSwitch luciferase assay system (SwitchGear Genomics S720355) was used per the manufactures protocol. Briefly, a mixture containing FuGENE 6 transfection reagent, 50ng Luciferase GoClone *CCNE1* promoter (#S720355) plasmid DNA, 50ng of either control (empty) vector or CIC-DUX4 or wild-type CIC was added to each well. All transfections were performed in quintuplicate.

Western blot analysis. All immunoblots represent at least two independent experiments. Adherent cells were washed and lysed with RIPA buffer supplemented with proteinase and phosphatase inhibitors. Proteins were separated by SDS-PAGE, transferred to Nitrocellulose membranes, and blotted with antibodies recognizing: CIC (Acris/Origene AP50924PU-N), GFP (Cell Signaling #2956), HSP90 (Cell Signaling #4877), ETV4 (Lifespan LS-B1527), CCNE1 (Cell Signaling #20808), PARP (Cell Signaling #9532), Phosphor-RB (Cell Signaling), Actin (Sigma Clone AC-74), HA-tag (Cell Signaling #2367).

Real-Time Quantitative Polymerase Chain Reaction (RT-Q-PCR)

Isolation and purification of RNA was performed using RNeasy Mini Kit (Qiagen). 500 ng of total RNA was used in a reverse transcriptase reaction with the SuperScript III first-strand synthesis system (Invitrogen). Quantitative PCR included four replicates per cDNA sample. Human (*CDK1, CDK2, CDK7, CDK9 CCNE1, CCNE2, ETV1, ETV4, ETV5, GAPDH*, and *TBP)* and mouse (*CCNE1*, *CCNE2*, and *GAPDH*) were amplified with Taqman gene expression assays (Applied Biosystems). Expression data was acquired using an ABI Prism 7900HT

Sequence Detection System (Applied Biosystems). Expression of each target was calculated using the $2^{-\Delta\Delta Ct}$ method and expressed as a relative mRNA expression.

Transwell migration and invasion assays. RPMI with 10% FBS was added to the bottom well of a trans-well chamber. $2.5x10^4$ cells resuspended in serum free media was then added to the top 8 μM pore matrigel coated (invasion) or non-coated (migration) trans-well insert (BD Biosciences). After 20 hours, non-invading cells on the apical side of inserts were scraped off and the trans-well membrane was fixed in methanol for 15 minutes and stained with Crystal Violet for 30 minutes. The basolateral surface of the membrane was visualized with a Zeiss Axioplan II immunofluorescent microscope at 10X. Each trans-well insert was imaged in five distinct regions at 10X and performed in triplicate. % invasion was calculated by dividing the mean # of cells invading through Matrigel membrane / mean # of cells migrating through control insert.

Xenograft tumors. Subcutaneous xenografts were explanted on day 4 of treatment. Tumor explants were immediately immersed in liquid nitrogen and stored at -80 degrees. Tumors were disrupted with a mortar and pestle, followed by sonication in RIPA buffer supplemented with proteinase and phosphatase inhibitors. Proteins were separated as above. Antibodies to PARP and phosphor-RB were both from Cell Signaling.

Establishment of a CIC responsive gene set and identification of CIC-DUX4 target genes. A publicly curated Affymetrix mRNA dataset (GSE60740) of 14

CIC-DUX4 tumors, 7 EWSR1-NFATc2 tumors, and a CIC-DUX4 expressing cell line (IB120) expressing either shRNA's targeting CIC-DUX4 or control was used to generate a list of CIC-DUX4 responsive genes. Notably, the entire dataset was profiled on the same Affymetrix Human Genome U133 Plus 2.0 array, enabling a direct comparison between tumor types. We first independently compared IB120 cells expressing either EV control to each individual shRNA targeting the CIC-DUX4 fusion (shCIC-DUX4a and shCICDUX4b). Using logFC<-2 and FDR<0.05, we identified 409 (shCIC-DUX4a) and 205 (shCIC-DUX4b) downregulated genes, respectively. We then generated a shared gene list (N = 165) of downregulated genes that we referred to as "CIC-DUX4 responsive genes". We then used the CIC-DUX4 responsive gene set to perform functional clustering with Database for Annotation, Visualization, and Integrated Discovery (DAVID). We performed a similar analysis using logFC>2 and FDR<0.05 to identify 286 (shCIC-DUX4a) and 168 (shCIC-DUX4b) upregulated genes, respectively. There were 105 upregulated genes that were shared between these two datasets.

Using the CIC-DUX4 responsive gene set, we generated a gene expression heat map comparing: 1) IB120 cells expressing control vector and; 2) the two independent shRNAs targeting CIC-DUX4; 3) the 14 CIC-DUX4 patient derived tumors and; 4) the 7 EWSR1-NFATc2 tumors. Hierarchical clustering was performed using the differentially expressed CIC-DUX4 responsive gene set. We performed a similar hierarchical comparison of PAX3-FOXO1 positive cell lines (RH30) to CIC-DUX4 positive NCC_CDS_X1 cells as documented above. The PAX3-FOXO1 (RH30) and CIC-DUX4 (NCC_CDS_X1) cells were sequenced on the same RNAseq platform, enabling a direct comparison between the gene sets.

To identify putative CIC-DUX4 target genes, we surveyed all 165 CIC responsive genes for the CIC-binding motifs (TG/CAATGA/GA) within -2000bp and +150bp of the transcriptional start site. 43 of the 165 genes contained the CIC-binding motif. Human promoter sequences were downloaded from eukaryotic promoter database (http://epd.vital-it.ch/).

Cell cycle analysis. To determine the effect of CIC-DUX4 expression on cell cycle, NIH-3T3 cell lines were cultured to ~70% confluence and transfected with CIC-DUX4 or a GFP control vector for 48 hours. Cells were trypsinized and fixed in ice cold ethanol for 10 minutes and subsequently stained with propidium iodide (PI) solution (Sigma Aldrich) at room temperature for 15 minutes. Cells were analyzed on a BD LSRII flow cytometer.

Statistical analysis. Experimental data are presented as mean +/- SEM. P-values derived for all in-vitro experiments were calculated using two-tailed Student's t test or one-way ANOVA. A P-value <0.05 was considered statistically significant.

Study approval. For tumor xenograft studies, including orthotopic and subcutaneous models, specific pathogen-free conditions and facilities were approved by the American Association for Accreditation of Laboratory Animal Care. Surgical procedures were reviewed and approved by the UCSF Institutional Animal Care and Use Committee (IACUC), protocol #AN107889-03A.

Supplemental Figure 1. CIC-DUX4 promotes invasion and metastasis through ETV4

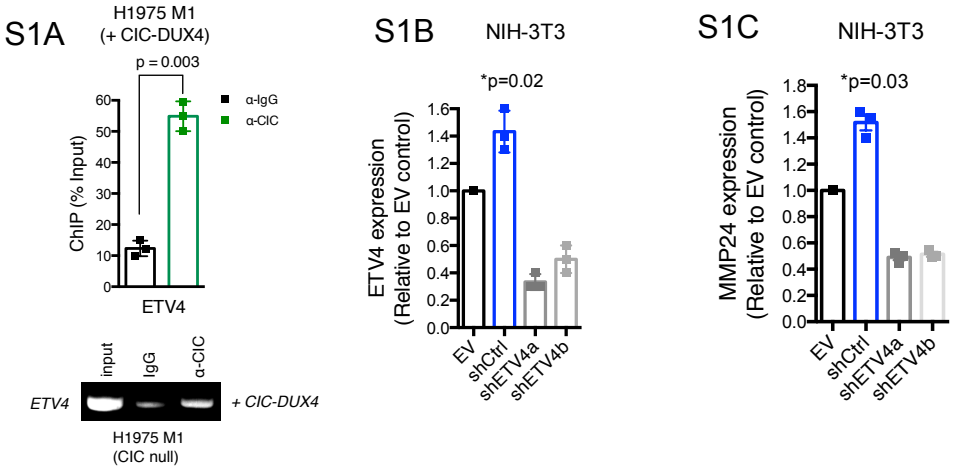

Supplemental Figure 1. CIC-DUX4 promotes invasion and metastasis through ETV4

A) ChIP-PCR from H1975 M1 (CIC wild-type null) cells reconstituted with CIC-DUX4 showing CIC-DUX4 occupancy on the *ETV4* promoter. ETV4 (B) and MMP24 (C) protein expression in NIH-3T3 cells expressing either EV or CIC-DUX4 with shCtrl, shETV4a, or shETV4b. Performed in triplicate and quantified using Image J software.

Supplemental Figure 2. CIC-DUX4 regulates cell-cycle progression and tumor growth.

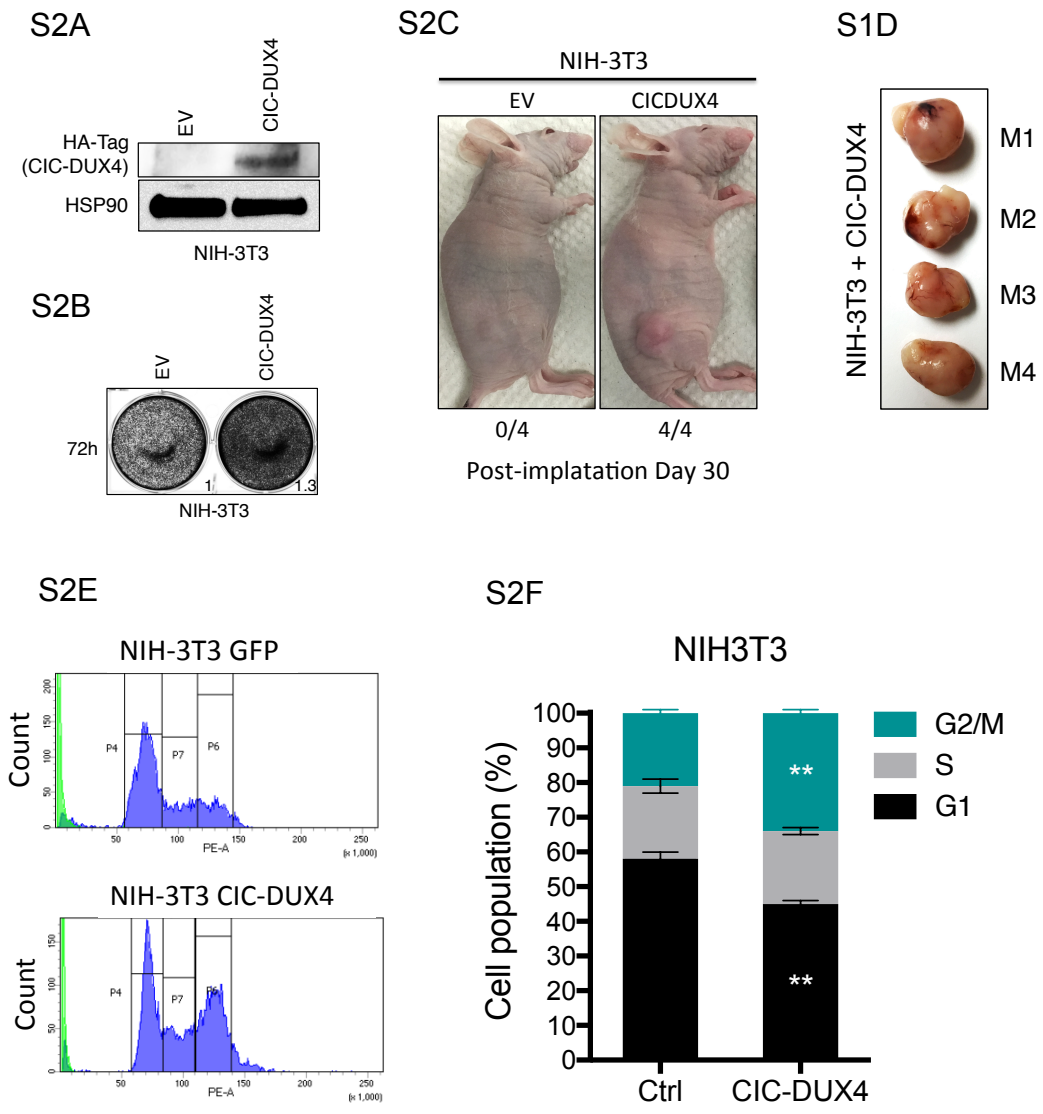

Supplemental Figure 2. CIC-DUX4 regulates cell-cycle progression and tumor growth

A) Immunoblot of CIC-DUX4 (HA-tag) and HSP90 in NIH-3T3 cells. B) Crystal violet assay comparing NIH-3T3 cells expressing either EV control or CIC-DUX4. C) Subcutaneously implanted NIH-3T3 cells expressing either EV control (n=4) or CIC-DUX4 (n=4). D) Tumor explants from mice in S2C. E) Cell-cycle profiles of NIH-3T3 cells expressing GFP control (top) or CIC-DUX4 (bottom). F) Cell-cycle distribution of NIH-3T3 cells expressing either EV control or CIC-DUX4 alone. Performed in triplicate. **p-value = <0.005. Error bars represent SEM.

Supplemental Figure 3. CCNE1 inhibition decreases tumor growth in CIC-DUX4 expressing cells.

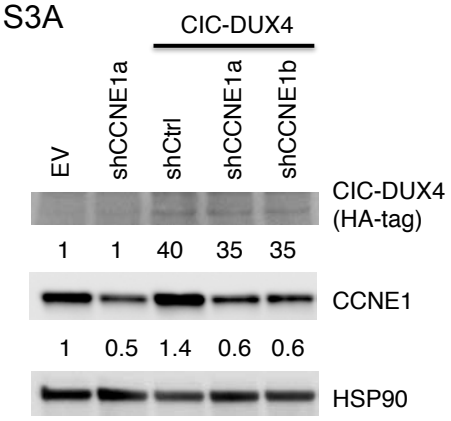

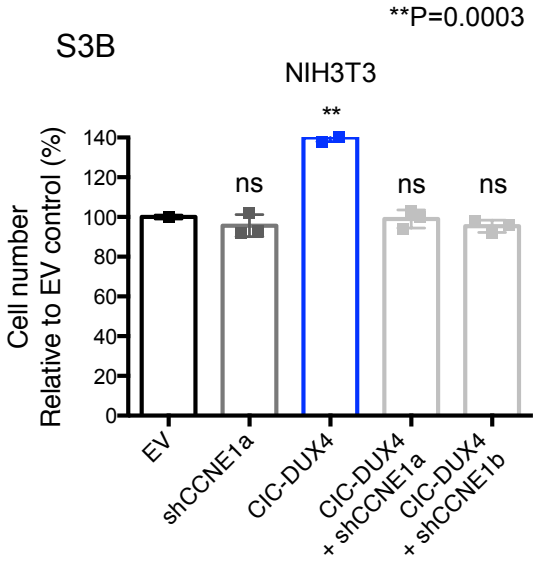

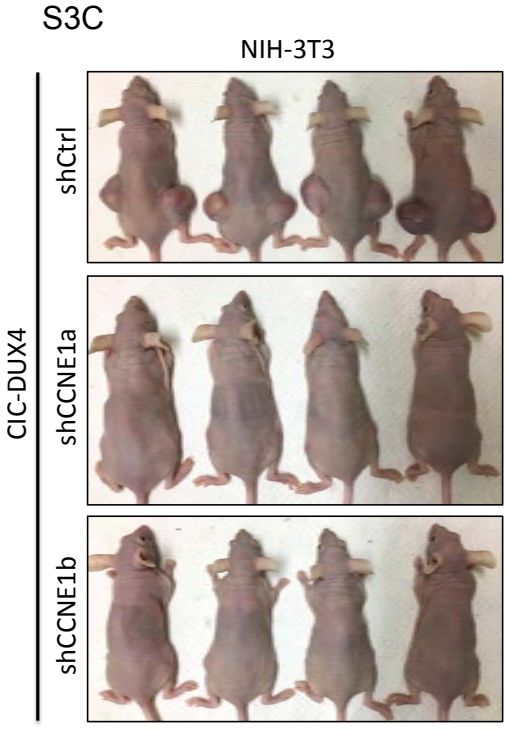

Supplemental Figure 3. CCNE1 inhibition decreases tumor growth in CIC-DUX4 expressing cells

A) Immunoblot of CIC-DUX4 (HA-Tag), CCNE1, and HSP90 in NIH-3T3 cells. B) Relative cell number of NIH-3T3 cells expressing either EV, shCCNE1a, CIC-DUX4 with or without shCCNE1a or shCCNE1b. **p-value = 0.0003. C) Subcutaneously implanted NIH-3T3 cells expressing CIC-DUX4 and either shCtrl, shCCNE1a, or shCCNE1b.

Supplemental Figure 4. ETV4, but not ETV1 or ETV5 controls CIC-DUX4 mediated invasion.

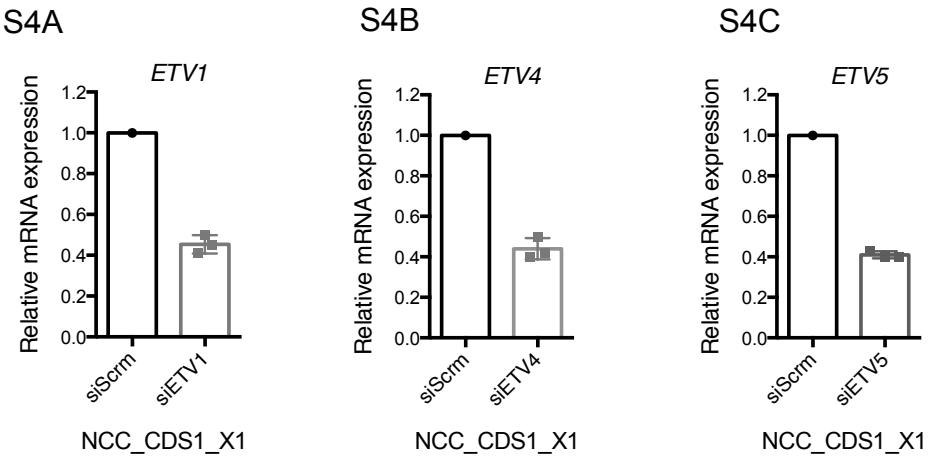

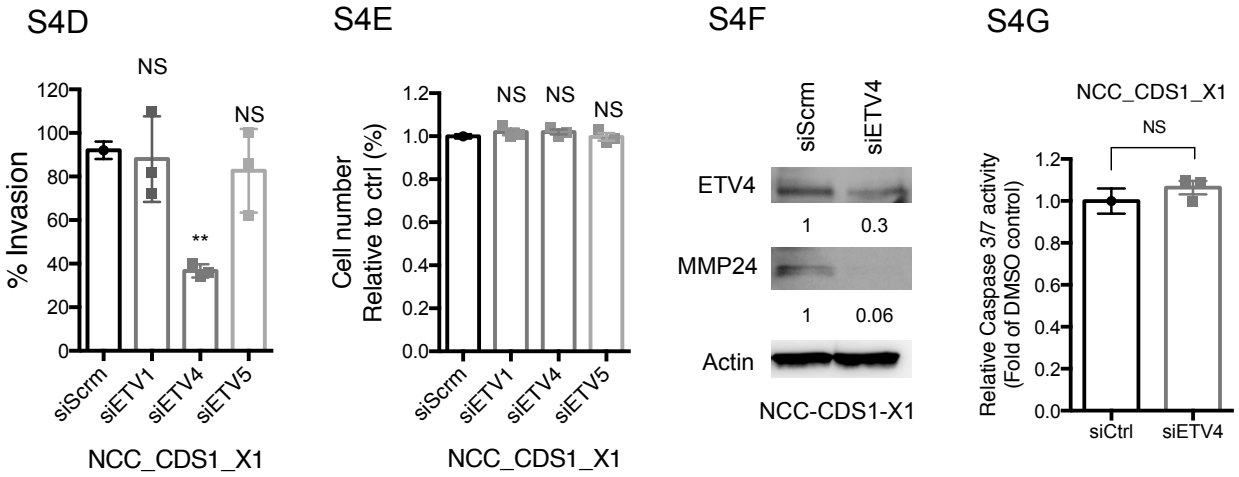

Supplement Figure 4. ETV4, but not ETV1 or ETV5 controls CIC-DUX4 mediated invasion

Relative *ETV1* (A), *ETV4* (B), and *ETV5* (C) mRNA expression in NCC_CDS1_X1 cells expressing either siETV1, siETV4, and siETV5 compared to siScrm. Performed in triplicate. Error bars represent SEM. D) Transwell invasion assay comparing NCC_CDS1_X1 cells expressing either siScrm, siETV1, siETV4, and siETV5. Performed in triplicate. Error bars represent SEM. E). Relative cell number of NCC_CDS1_X1 cells expressing either siScrm, siETV1, siETV4, and siETV5. Performed in triplicate. Error bars represent SEM. F) Immunoblot of ETV4 and MMP24 from NCC_CDS1_X1 cells expressing either siScrm control or siETV4. G) Relative caspase 3/7 activity in NCC_CDS1_X1 cells expressing either siScrm control or siETV4. Performed in triplicate. Error bars represent SEM.

Supplemental Figure 5. Pharmacologic inhibition of CDK2 with SNS-032 induces apoptosis in CIC-DUX4 expressing cells.

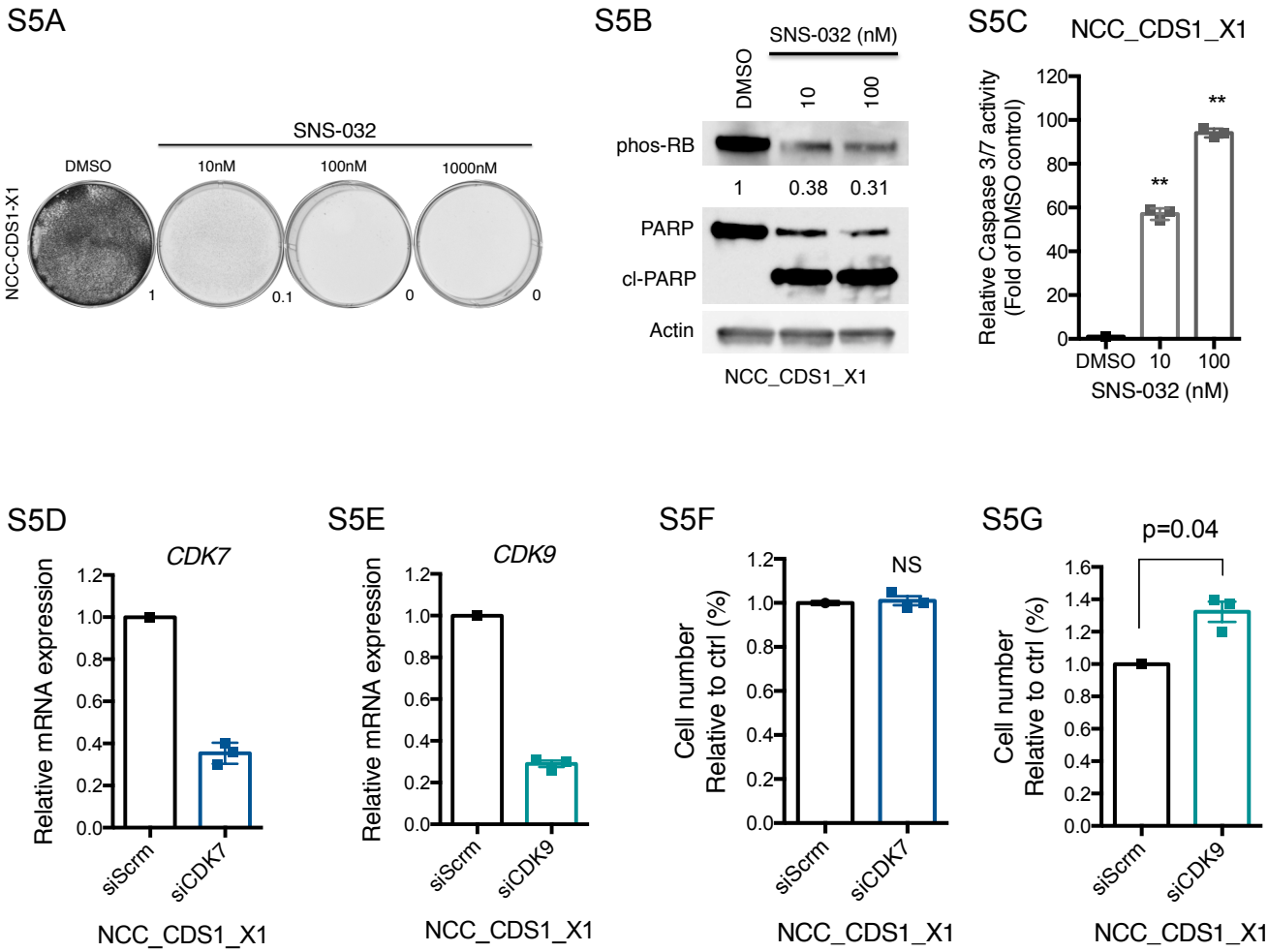

Supplemental Figure 5. Pharmacologic inhibition of CDK2 with SNS-032 induces apoptosis in CIC-DUX4 expressing cells

A) 72 hour crystal violet assay of NCC_CDS1_X1 cells treated with SNS-032. B) immunoblot of phosphorylated-Rb, PARP, and Actin from NCC_CDS_X1 cells treated with SNS-032 or DMSO. C) Relative caspase 3/7 activity in NCC_CDS1_X1 cells treated with SNS-032 or DMSO. **p-value < 0.0001, one-way ANOVA. Relative *CDK7* (D) and *CDK9* (E) mRNA expression in NCC_CDS1_X1 cells expressing either siScrm control, siCDK7, or siCDK9 respectively. Performed in triplicate. Error bars represent SEM. F) Relative cell number of NCC_CDS_X1 cells expressing either siScrm or siCDK7. Performed in triplicate. Error bars represent SEM. G) Relative cell number of NCC_CDS1_X1 cells expressing either siScrm or siCDK9. Performed in triplicate. Error bars represent SEM. P-values calculated by Student's T-test.

Supplemental Figure 6. The CCNE-CDK2 complex is a specific therapeutic target in CIC-DUX4 tumors.

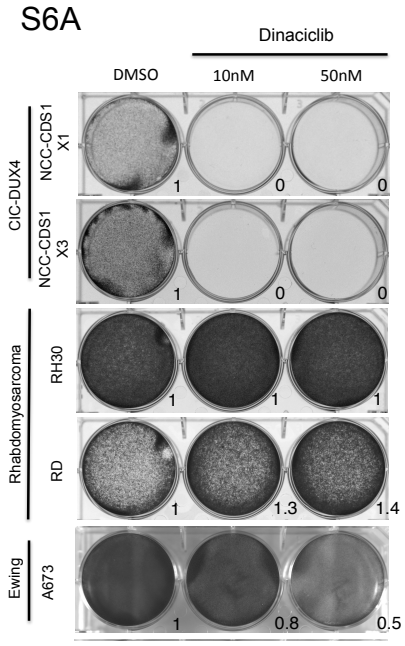

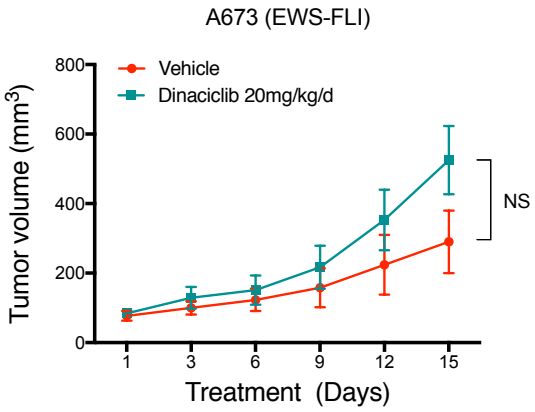

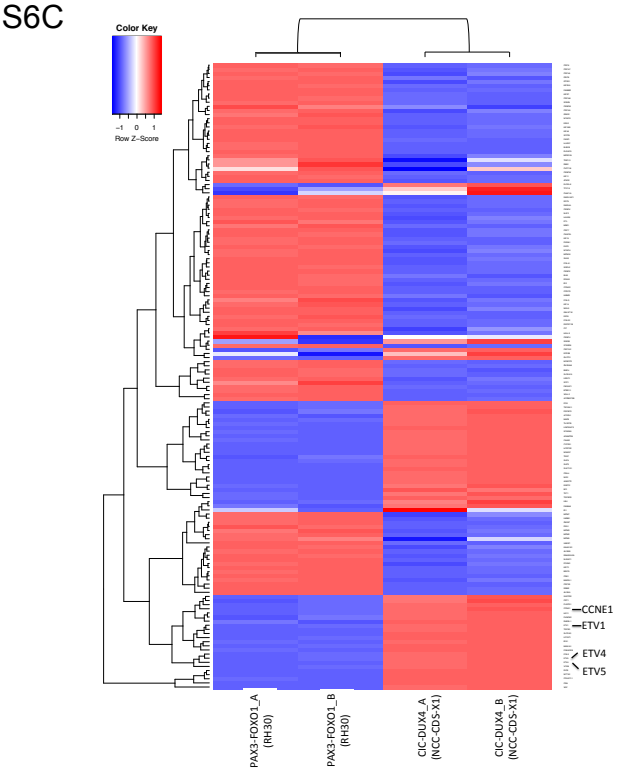

Supplemental Figure 6. The CCNE-CDK2 complex is a specific therapeutic target in CIC-DUX4 tumors

A) 72 hour crystal violet assay of CIC-DUX4 (NCC_CDS1_X1 and NCC_CDS1_X3), rhabdomyosarcoma (RD and RH30), Ewing sarcoma (A673) cells treated with vehicle or dinaciclib. B) Subcutaneously implanted Ewing sarcoma (A673) cells treated with either vehicle (n=6) or dinaciclib (n=6). Error bars represent SEM. C) Heatmap comparing 165 CIC-DUX4 activated genes identified in CIC-DUX4 expressing NCC-CDS1-X1 cells vs PAX3-FOXO1 containing RH30 cells. CCNE1, ETV1, ETV4, and ETV5 are magnified.

Supplemental Figure 7. Genetic inhibition of the CCNE-CDK2 complex decreases CIC-DUX4 tumor growth.

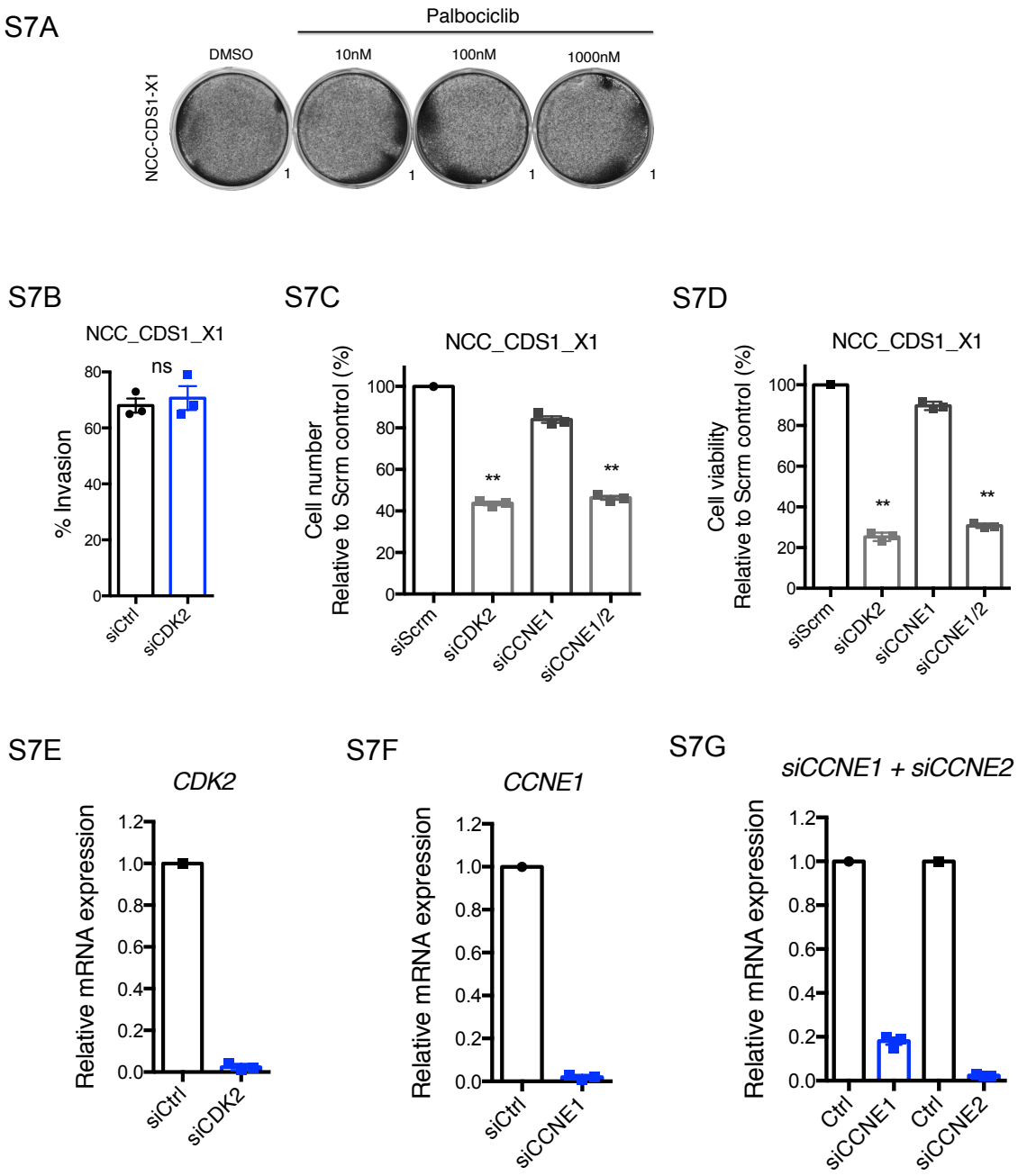

Supplemental Figure 7. Genetic inhibition of the CCNE-CDK2 complex decreases CIC-DUX4 tumor growth

A) Five day crystal violet assay of NCC_CDS1_X1 cells treated with palbociclib. B) Transwell invasion assay comparing CIC-DUX4 expressing NCC_CDS1_X1 cells with either siCtrl or siCDK2. Error bars represent SEM. C) Relative cell number of NCC_CDS1_X1 cells following knockdown of CDK2, CCNE1, and combination CCNE1 and CCNE2 compared to scramble control. **p-value = 0.0001, one-way ANOVA. Error bars represent SEM. D) Relative cell viability (cell titer glo assay) of NCC_CDS1_X1 cells following knockdown of *CDK2*, *CCNE1*, and combination *CCNE1* and *CCNE2* compared to scramble control. **p-value = 0.0001, one-way ANOVA. Error bars represent SEM. E) Relative mRNA expression following *CDK2* (E), *CCNE1* (F), or dual *CCNE1* and *CCNE2* (G) knockdown compared to scramble control. performed in triplicate. Error bars represent SEM.

Supplemental Figure 8. *CCNE1* is a conserved CIC-DUX4 target gene.

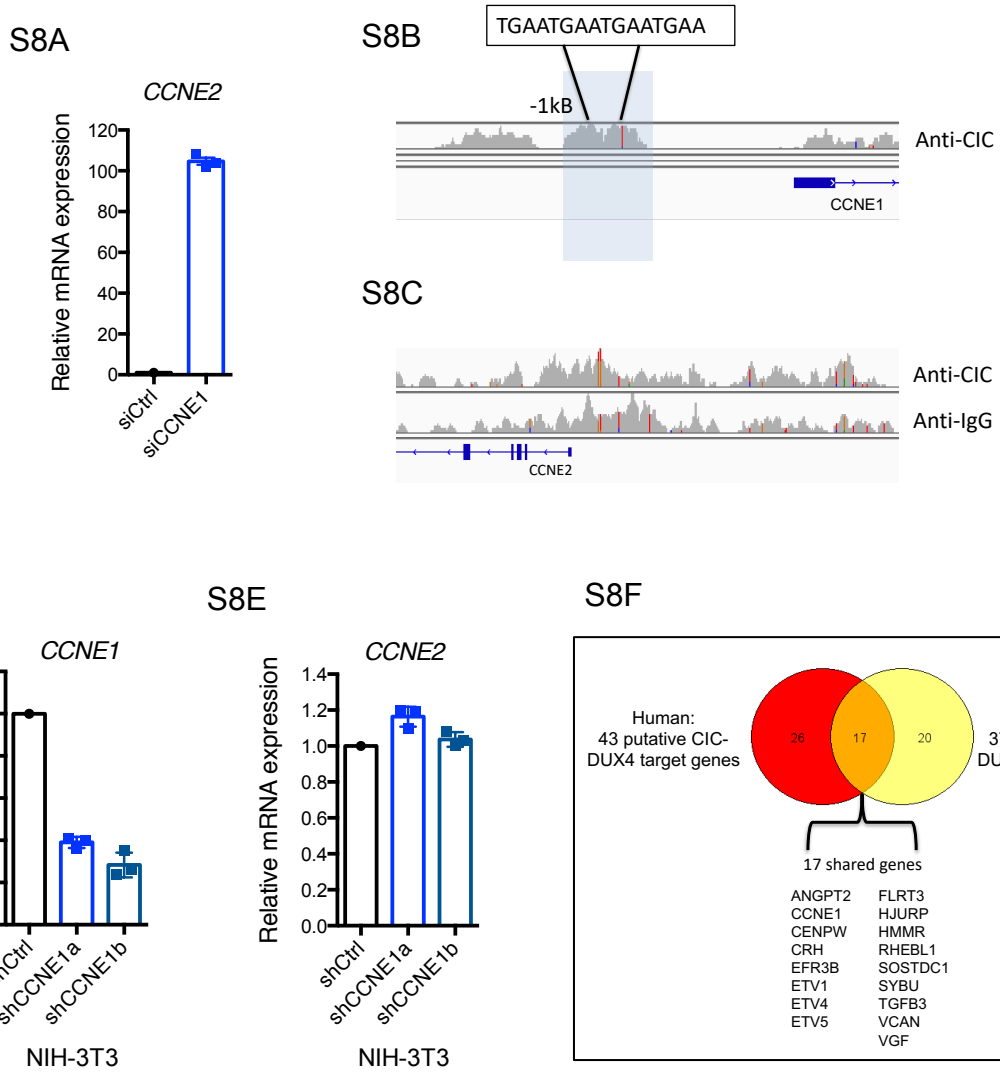

Supplemental Figure 8. *CCNE1* is a conserved CIC-DUX4 target gene

A) Relative *CCNE2* mRNA expression following *CCNE1* knockdown compared to scramble control in NCC_CDS1_X1 cells. B) CIC-DUX4 binding sites and ChIP-Seq peaks on the *CCNE1* promoter in NCC_CDS1_X1 cells. C) ChIP-Seq analysis of the CCNE2 promoter region comparing anti-CIC and anti-IgG immunoprecipitations. Relative *CCNE1* (D) and *CCNE2* (E) mRNA expression following *CCNE1* knockdown compared to scramble control in CIC-DUX4 expressing NIH-3T3 cells. Performed in triplicate. Error bars represent SEM. F) Venn diagram comparing human (n=43) and mouse (n=37) putative CIC-DUX4 targets demonstrating 17 shared genes.

Table S1. Downregulated genes upon CIC-DUX4 KD			
GeneSymbol	ID.x	adj.P.Val.x	logFC.x
ACVRL1	94_at	0.007062	-3.33
ADAMTS9	56999_at	0.031875	-2.59
AGR2	10551_at	0.04047	-2.39
ANGPT2	285_at	0.012833	-6.14
APOBEC3B	9582_at	0.012637	-4.44
ATAD2	29028_at	0.004162	-3.75
AURKA	6790_at	0.004515	-4.32
AURKB	9212_at	0.007277	-4.21
BIRC5	332_at	0.008102	-4.5
BLM	641_at	0.003109	-4.95
BMP4	652_at	0.023837	-2.33
BPI	671_at	0.003356	-3.16
BTBD11	121551_at	0.00563	-2.61
BUB1B	701_at	0.010978	-4.34
CALB2	794_at	0.012137	-4.42
CCDC3	83643_at	0.012416	-2.26
CCNE1	898_at	0.003636	-2.8
CCNE2	9134_at	0.005342	-4.54
CDC20	991_at	0.005393	-5.89
CDC45	8318_at	0.011462	-3.58
CDC6	990_at	0.004857	-4.91
CDC7	8317_at	0.006338	-3.34
CDCA5	113130_at	0.004319	-4.61
CDCA7	83879_at	0.010166	-2.53
CDCA8	55143_at	0.001873	-4.1
CDH4	1002_at	0.034988	-2.41
CDK1	983_at	0.003935	-4.76
CDT1	81620_at	0.007726	-3.61
CENPE	1062_at	0.011145	-5.25
CENPK	64105_at	0.006043	-3.38
CENPM	79019_at	0.00155	-4.27
CENPU	79682_at	0.004162	-4.18
CENPW	387103_at	0.012751	-3.86
CEP152	22995_at	0.009666	-2.51
CHAF1A	10036_at	0.003652	-3.26
CHTF18	63922_at	0.00155	-2.26
CIT	11113_at	0.002885	-4.09
CKAP2L	150468_at	0.008394	-4.29
COLEC11	78989_at	0.008331	-3.57
CRH	1392_at	0.011093	-3.61
CYP2S1	29785_at	0.010176	-2.04
DDIAS	220042_at	0.007279	-4
DEPDC1B	55789_at	0.011113	-4.63
DIO3	1735_at	0.004162	-6.6
DLGAP5	9787_at	0.022892	-5.46
DTL	51514_at	0.003109	-5.03
E2F8	79733_at	0.005526	-3.16
EFR3B	22979_at	0.008838	-2.94
ELOVL6	79071_at	0.005324	-3.2
ENPP2	5168_at	0.004882	-2.55
ETV1	2115_at	0.018832	-3.31
ETV4	2118_at	0.021186	-4.72
ETV5	2119_at	0.005048	-3.12
EXO1	9156_at	0.011245	-4.1
EZH2	2146_at	0.031747	-2.91
FAM64A	54478_at	0.020893	-6.69
FAM83D	81610_at	0.002189	-4.52
FANCI	55215_at	0.008394	-3.8
FEN1	2237_at	0.007656	-2.91
FGFBP3	143282_at	0.006618	-2.46
FIGNL1	63979_at	0.004486	-2.1
FLRT3	23767_at	0.003727	-2.25
FOS	2353_at	0.00463	-4.18
FOXM1	2305_at	0.011748	-5.11
GALNT16	57452_at	0.005088	-5.62
GINS2	51659_at	0.007521	-4.47
GLCCI1	113263_at	0.00976	-2.14
GTSE1	51512_at	0.006618	-4.04
HAUS8	93323_at	0.013919	-2.9
HCRTR2	3062_at	0.004162	-5.45
HELLS	3070_at	0.004486	-3.56
HEY1	23462_at	0.003927	-4.1
HJURP	55355_at	0.025418	-5.11
HMMR	3161_at	0.003877	-5.53
ID1	3397_at	0.00472	-2.57
ID2	3398_at	0.002189	-3.2
IL18R1	8809_at	0.008314	-4.7
IRX1	79192_at	0.00363	-2.73
KIAA0101	9768_at	0.003356	-4.75
KIF11	3832_at	0.004515	-3.82
KIF14	9928_at	0.004083	-4.44
KIF15	56992_at	0.007378	-4.13
KIF18B	146909_at	0.005006	-4.4

GeneSymbol	ID.x	adj.P.Val.x	logFC.x
KIF20A	10112_at	0.009833	-5.66
KIF2C	11004_at	0.005093	-4.16
KIF4A	24137_at	0.009833	-5.44
KIFC1	3833_at	0.009228	-3.94
LBH	81606_at	0.040084	-2.48
LHX1	3975_at	0.028595	-2.46
LINC00473	90632_at	0.001154	-4.96
LINC00911	100996280_at	0.009146	-2.55
LMNB1	4001_at	0.00463	-4.74
LOC100506718	100506718_at	0.003575	-3.92
LPCAT1	79888_at	0.004857	-3.07
LRRC1	55227_at	0.003109	-2.11
MAD2L1	4085_at	0.008314	-3.86
MAFB	9935_at	0.003784	-2.73
MAN1A1	4121_at	0.010507	-2.58
MCM10	55388_at	0.003109	-4.5
MCM2	4171_at	0.013357	-3.68
MCM3	4172_at	0.004162	-2.67
MCM5	4174_at	0.010507	-2.87
MCM7	4176_at	0.011905	-2.83
MFSD2A	84879_at	0.005205	-3.17
MND1	84057_at	0.002189	-4
MYBPC2	4606_at	0.007542	-3.54
MYH13	8735_at	0.029464	-2.44
MYH8	4626_at	0.040752	-2.37
NCAPG	64151_at	0.013519	-4.6
NCAPH	23397_at	0.005479	-5.27
NEIL3	55247_at	0.001154	-3.99
NID2	22795_at	0.002189	-4.01
NPTX2	4885_at	0.009557	-3.3
NRARP	441478_at	0.042544	-3.04
NUF2	83540_at	0.005212	-4.83
NUSAP1	51203_at	0.013043	-5.16
ORC6	23594_at	0.003432	-3.52
PCSK1	5122_at	0.001325	-6.01
PIK3AP1	118788_at	0.005009	-4.42
PKNOX2	63876_at	0.004316	-3.14
PLSCR1	5359_at	0.003356	-3.55
POLA1	5422_at	0.030571	-2.74
POLE	5426_at	0.008477	-6.38
POLE2	5427_at	0.003356	-4.21
POLQ	10721_at	0.012423	-4.37
PRICKLE1	144165_at	0.026937	-2.05
PRKAR2B	5577_at	0.009036	-2.87
RAD51AP1	10635_at	0.008116	-3.51
RAD54L	8438_at	0.005324	-3.32
RFC5	5985_at	0.006166	-3.59
RHEBL1	121268_at	0.007408	-2.99
RMI2	116028_at	0.018761	-3.81
RNASEH2A	10535_at	0.006572	-4.2
RRM2	6241_at	0.004316	-5.01
SAPCD2	89958_at	0.002189	-5.37
SCARA5	286133_at	0.003356	-3.02
SGOL2	151246_at	0.001154	-3.99
SHC3	53358_at	0.003636	-3.61
SHC4	399694_at	0.003968	-2.6
SKA3	221150_at	0.006618	-3.09
SLC2A3	6515_at	0.003652	-2.34
SLC6A15	55117_at	0.003356	-3.88
SNX30	401548_at	0.002612	-2.16
SOSTDC1	25928_at	0.009789	-2.29
SPAG5	10615_at	0.010978	-5.39
SPC25	57405_at	0.005529	-4.56
SPP1	6696_at	0.004882	-4.6
STARD8	9754_at	0.009054	-3.07
SULT1E1	6783_at	0.003567	-4.15
SYBU	55638_at	0.010005	-3.29
TCF19	6941_at	0.008106	-4.08
TESC	54997_at	0.018179	-2.5
TET1	80312_at	0.003575	-3.26
TGFB3	7043_at	0.012097	-3.59
TGFBR3	7049_at	0.002885	-4.52
THSD7B	80731_at	0.024784	-2.91
TRIP13	9319_at	0.009126	-3.57
TSPAN11	441631_at	0.003655	-2.84
TYRP1	7306_at	0.014058	-2.19
UBE2C	11065_at	0.013755	-4.68
VCAN	1462_at	0.003216	-2.64
VGF	7425_at	0.02702	-2.02
VGLL2	245806_at	0.012671	-2.88
ZNF804A	91752_at	0.010166	-3.97
ZWINT	11130_at	0.004826	-4.51

Table S2. Upregulated genes upon CIC-DUX4 KD			
GeneSymbol	ID.x	adj.P.Val.x	logFC.x
ABI3BP	25890_at	0.011435	3.71
ADAM12	8038_at	0.004483	3.62
ADAMTS6	11174_at	0.002189	3.08
AGO3	192669_at	0.020917	2.1
AOX1	316_at	0.002004	4.48
ARL4C	10123_at	0.00155	6.02
ARNT2	9915_at	0.034627	2.12
ATP8B1	5205_at	0.010206	3.62
ATP9A	10079_at	0.013976	2.31
C14orf28	122525_at	0.007866	3.64
C15orf48	84419_at	0.001325	5.51
C2CD2	25966_at	0.007278	2.87
C3AR1	719_at	0.002994	3.6
C3orf52	79669_at	0.010507	2.31
CA8	767_at	0.009272	2.08
CARD6	84674_at	0.00946	2.01
CD274	29126_at	0.005144	5.49
CEMIP	57214_at	0.000776	6.45
CEMIP2	23670_at	0.009444	3.72
CLDN1	9076_at	0.003221	5.57
COL1A1	1277_at	0.007378	3.2
COL3A1	1281_at	0.012092	3.23
COLEC12	81035_at	0.002885	3.83
CPA3	1359_at	0.0032	3.03
CTHRC1	115908_at	0.004515	3.76
CYP24A1	1591_at	0.018761	2.72
DKK1	22943_at	0.003356	3.86
DUBR	344595_at	0.014541	2.67
DUSP3	1845_at	0.00463	2.76
EDN1	1906_at	0.009119	7.26
EGR1	1958_at	0.001325	2.74
ELL2	22936_at	0.003356	2.01
FGF1	2246_at	0.016402	2.21
FILIP1L	11259_at	0.003567	4.48
FRMD6	122786_at	0.011341	2.62
FST	10468_at	0.016401	2.88
GAPLINC	100505592_at	0.008105	4.72
GAS6	2621_at	0.001325	3.46
GBP1	2633_at	0.005038	3.14
GBP2	2634_at	0.015941	3.69
GDF15	9518_at	0.003833	4.01
GLIPR1	11010_at	0.006676	2.8
GLS	2744_at	0.006551	2.22
GLT8D2	83468_at	0.006474	2.67
HHAT	55733_at	0.015729	2.72
HIST1H1C	3006_at	0.009715	2.61
HIST1H4H	8365_at	0.01762	2.9
HMOX1	3162_at	0.002539	4.04
HOXC6	3223_at	0.011744	2.02
HTR2B	3357_at	0.001921	6.44
IGFBP3	3486_at	0.007468	4.13
IGFBP5	3488_at	0.011744	3.68
IGFBP7	3490_at	0.002885	6.37
KCTD12	115207_at	0.002562	2.98
KRTAP2-3	730755_at	0.000776	7.95
LAMB3	3914_at	0.028202	3.73
LINC00460	728192_at	0.016475	4.54
LOC151760	151760_at	0.019194	2.14
LRRC17	10234_at	0.008883	4.18
LTBP2	4053_at	0.015508	2.32
LYPD6B	130576_at	0.003948	3.4
MAP3K7CL	56911_at	0.006045	5.04
C3HC4	57574_at	0.003609	3.91
MBNL1-AS1	401093_at	0.004162	3.5
MGLL	11343_at	0.022738	3.16
MMP3	4314_at	0.007666	3.63
MOK	5891_at	0.014633	3.1
MOXD1	26002_at	0.010302	3.95
MSTN	2660_at	0.004395	4.97
MYBL1	4603_at	0.006166	2.15
MYLK	4638_at	0.003425	2.85
MYO1E	4643_at	0.007754	3.22
MYOF	26509_at	0.007773	2.67
NABP1	64859_at	0.005731	3.21
NEDD4	4734_at	0.012185	2.45
NMRK1	54981_at	0.018801	3.34
NOG	9241_at	0.003786	5.68
OLFML3	56944_at	0.026353	2.08
OPTN	10133_at	0.002189	2.45
OXTR	5021_at	0.004832	5.81
PALMD	54873_at	0.002189	2.35
PLA2G4C	8605_at	0.003257	4.86
PLAT	5327_at	0.0216	3.99
PLAU	5328_at	0.008102	5.58
POSTN	10631_at	0.004316	3.59
PSG4	5672_at	0.017603	3.78
PSG5	5673_at	0.011842	4.25
PTPRJ	5795_at	0.004515	2.59
RCAN1	1827_at	0.041172	3.44
RGS7	6000_at	0.004882	3.62
S100A2	6273_at	0.003567	2.44
SCG5	6447_at	0.002521	3.41
SERPINE1	5054_at	0.019986	4.8
SLC22A4	6583_at	0.001154	4.19
SULF1	23213_at	0.008102	3.37
SYTL2	54843_at	0.010628	2.77
TGFBI	7045_at	0.021631	4.2
TIPARP	25976_at	0.003356	2.76
TMEM154	201799_at	0.008612	3.03
TMEM200A	114801_at	0.003784	4.91
TMEM40	55287_at	0.001154	5.42
TNFRSF11B	4982_at	0.000776	5.89
TPD52L1	7164_at	0.004634	2.7
WNT5B	81029_at	0.002019	3.7
ZYX	7791_at	0.019158	2.43

Table S3. Putative CIC-DUX4 target genes - human		
GeneSymbol	ID	Description
ANGPT2	285_at	angiopoietin 2
BLM	641_at	Bloom syndrome, RecQ helicase-like
CCNE1	898_at	cyclin E1
CDC45	8318_at	cell division cycle 45
CENPE	1062_at	centromere protein E, 312kDa
CENPM	79019_at	centromere protein M
CENPW	387103_at	centromere protein W
CRH	1392_at	corticotropin releasing hormone
CYP2S1	29785_at	cytochrome P450, family 2, subfamily S, polypeptide 1
DLGAP5	9787_at	discs, large (Drosophila) homolog-associated protein 5
EFR3B	22979_at	EFR3 homolog B (S. cerevisiae)
ELOVL6	79071_at	ELOVL fatty acid elongase 6
ETV1	2115_at	ets variant 1
ETV4	2118_at	ets variant 4
ETV5	2119_at	ets variant 5
FAM83D	81610_at	family with sequence similarity 83, member D
FANCI	55215_at	Fanconi anemia, complementation group I
FGFBP3	143282_at	fibroblast growth factor binding protein 3
FLRT3	23767_at	fibronectin leucine rich transmembrane protein 3
GLCCI1	113263_at	glucocorticoid induced transcript 1
GTSE1	51512_at	G-2 and S-phase expressed 1
HELLS	3070_at	helicase, lymphoid-specific
HJURP	55355_at	Holliday junction recognition protein
HMMR	3161_at	hyaluronan-mediated motility receptor (RHAMM)
KIF4A	24137_at	kinesin family member 4A
KIFC1	3833_at	kinesin family member C1
MAD2L1	4085_at	MAD2 mitotic arrest deficient-like 1 (yeast)
MCM10	55388_at	minichromosome maintenance complex component 10
MCM7	4176_at	minichromosome maintenance complex component 7
NEIL3	55247_at	nei endonuclease VIII-like 3 (E. coli)
PKNOX2	63876_at	PBX/knotted 1 homeobox 2
POLQ	10721_at	polymerase (DNA directed), theta
RAD51AP1	10635_at	RAD51 associated protein 1
RHEBL1	121268_at	Ras homolog enriched in brain like 1
RRM2	6241_at	ribonucleotide reductase M2
SOSTDC1	25928_at	sclerostin domain containing 1
SULT1E1	6783_at	sulfotransferase family 1E, estrogen-preferring, member 1
SYBU	55638_at	syntabulin (syntaxin-interacting)
TGFB3	7043_at	transforming growth factor, beta 3
TGFBR3	7049_at	transforming growth factor, beta receptor III
VCAN	1462_at	versican
VGF	7425_at	VGF nerve growth factor inducible
ZWINT	11130_at	ZW10 interactor, kinetochore protein

Table S4. Putative CIC-DUX4 target genes - mouse		
GeneSymbol	ID	Description
ANGPT2	285_at	angiopoietin 2
ATAD2	29028_at	ATPase family, AAA domain containing 2
AURKB	9212_at	aurora kinase B
BTBD11	121551_at	BTB (POZ) domain containing 11
CCNE1	898_at	cyclin E1
CENPU	79682_at	MLF1 interacting protein
CENPW	387103_at	centromere protein W
CHAF1A	10036_at	chromatin assembly factor 1, subunit A (p150)
CIT	11113_at	citron (rho-interacting, serine/threonine kinase 21)
CKAP2L	150468_at	cytoskeleton associated protein 2-like
CRH	1392_at	corticotropin releasing hormone
DEPDC1B	55789_at	DEP domain containing 1B
EFR3B	22979_at	EFR3 homolog B (S. cerevisiae)
ETV1	2115_at	ets variant 1
ETV4	2118_at	ets variant 4
ETV5	2119_at	ets variant 5
FLRT3	23767_at	fibronectin leucine rich transmembrane protein 3
FOS	2353_at	FBJ murine osteosarcoma viral oncogene homolog
HJURP	55355_at	Holliday junction recognition protein
HMMR	3161_at	hyaluronan-mediated motility receptor (RHAMM)
IL18R1	8809_at	interleukin 18 receptor 1
KIF18B	146909_at	kinesin family member 18B
MCM5	4174_at	minichromosome maintenance complex component 5
MYH13	8735_at	myosin, heavy chain 13, skeletal muscle
NID2	22795_at	nidogen 2 (osteonidogen)
ORC6	23594_at	origin recognition complex, subunit 6
PRICKLE1	144165_at	prickle homolog 1 (Drosophila)
RHEBL1	121268_at	Ras homolog enriched in brain like 1
SCARA5	286133_at	scavenger receptor class A, member 5 (putative)
SHC4	399694_at	SHC (Src homology 2 domain containing) family, member 4
SOSTDC1	25928_at	sclerostin domain containing 1
SYBU	55638_at	syntabulin (syntaxin-interacting)
TESC	54997_at	tescalcin
TGFB3	7043_at	transforming growth factor, beta 3
TSPAN11	441631_at	tetraspanin 11
VCAN	1462_at	versican
VGF	7425_at	VGF nerve growth factor inducible